Article

Antioxidant and UV-Blocking Functionalized Poly(Butylene Succinate) Films

Serena Coiai [1],*, Nicola Migliore [1], Elisa Passaglia [1], Roberto Spiniello [1], Cristian Gambarotti [2] and Francesca Cicogna [1]

[1] Institute of Chemistry of Organometallic Compounds (ICCOM-CNR), SS Pisa, Via Moruzzi 1, 56124 Pisa, Italy
[2] Department of Chemistry, Materials and Chemical Engineering "Giulio Natta", Politecnico di Milano, Piazza Leonardo da Vinci 32, 20133 Milan, Italy
* Correspondence: serena.coiai@pi.iccom.cnr.it; Tel.: +39-050-315-2556

Abstract: The introduction of a limited number of functional groups on poly(butylene succinate) (PBS) chains by covalent bonding can impart new properties to the polymer without modifying its thermal and mechanical properties. In pursuit of a viable approach to obtain light- and heat-stabilized PBS samples, the nitroxide radical coupling (NRC) reaction between PBS macroradicals and the 3,5-di-tert-butyl-4-hydroxybenzoyl-2,2,6,6-tetramethylpiperidine-1-oxyl radical (BHB-TEMPO), a functionalizing agent bearing a sterically-hindered antioxidant phenol moiety, is here proposed. The reaction was initiated by peroxide and carried out in solution and in a melt. The functionalized materials were characterized by UV-visible spectroscopy (UV-Vis), proton nuclear magnetic resonance (^{1}H-NMR), and size exclusion chromatography (SEC) analysis to gain structural information and by thermal gravimetric analysis (TGA) and differential scanning calorimetry (DSC) to investigate the thermal properties. In addition, films of the samples were subjected to thermal and photo-oxidative aging to assess their resistance to degradative processes. Finally, the PBS film with the highest degree of functionalization showed the ability to protect β-carotene, a molecule found in food and drugs and that is very sensitive to UV light, from degradation. This result suggests the use of this material (either alone or blended with other biopolyesters) for biodegradable and compostable active packaging.

Keywords: poly(butylene succinate); nitroxide radical coupling; anti-oxidant; UV-blocking

1. Introduction

Aliphatic biopolyesters are among the most promising substitutes for conventional polymers of petrochemical origin since they are produced mainly from renewable sources and contain hydrolysable ester bonds that make them biodegradable or compostable [1,2]. Poly(butylene succinate) (PBS), in particular, is a valid alternative for the production of rigid and flexible short life-cycle packaging, usually made of polyolefins [3,4]. PBS can be derived from fossil or renewable sources, including cellulose, starch-based biomass, and glycerol [5–7]. It has a high thermal deflection temperature, it can be used in contact with food, and it is biocompatible, thus enabling possible biomedical applications [3].

Often, the insertion of new functional groups on polymer chains is necessary to achieve specific material properties (optical, antimicrobial, antioxidant, etc.) or to prepare polymer blends, coupled films, composites, and nanocomposites. In the case of polyesters, these modifications can be made at the polymerization stage, although with complex and expensive syntheses [8]. Therefore, post-polymerization functionalization, which involves radical modification with peroxides and unsaturated monomers, is preferable because it does not modify the polymer synthesis but only its subsequent transformation, using processes and machines that are commonly-available in the polymer compounding industry [9,10]. Although the classical radical functionalization reactions that use peroxide and unsaturated functional monomers, such as maleic anhydride, are largely applied to polyolefins, the same process, extended to biodegradable aliphatic polyesters, such as

poly(lactic acid) (PLA) and PBS, results in a whole series of side reactions [11,12]. These reactions generally lead to the degradation of the material from the point of view of rheological, thermal, and mechanical behavior [13–17]. In the last few years, our research group has developed a successful post-polymerization functionalization procedure for PLA and PBS [18,19]. The method works via a nitroxide radical coupling (NRC) reaction between 2,2,6,6-tetramethyl piperidinyl-1-oxyl (TEMPO) derivatives bearing different functionalities and the macroradicals generated by H-abstraction using a peroxide (Scheme 1) [20–23].
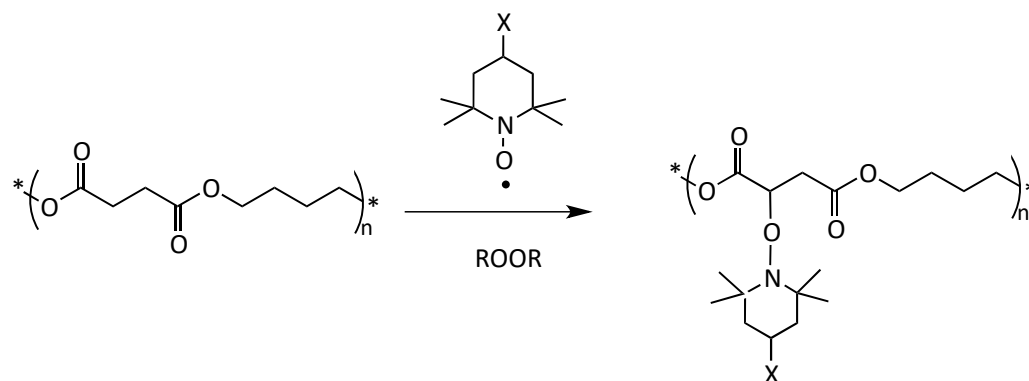

Scheme 1. Simplified mechanism of grafting of a functional TEMPO derivative onto a PBS polymer chain with a peroxide (ROOR) as initiator.

The NRC reaction has several advantages, including that it is generally robust and highly tolerant towards functional groups [20]. PBS and PLA, for example, were functionalized with 4-benzoyloxy-2,2,6,6-tetramethylpiperidine-1-oxyl (BzO-TEMPO) and 4-(1-naphthoate)-2,2,6,6-tetramethylpiperidine-1-oxyl (NfO-TEMPO), achieving an excellent level of grafting and an efficient control of radical-induced polymer substrate cross-linking/branching side reactions, thus preserving the initial characteristics of the material [18,24].

As previously mentioned, the functionalization of a polymer matrix can improve some of the material's properties, such as the material's resistance to thermal and UV-induced degradation, which is particularly important in food packaging applications. Indeed, due to light and temperature, polymers are generally subjected to oxidative degradation during their processing and service life. PBS also exhibits poor resistance to degradation by UV irradiation and high transmittance to ultraviolet (UV) light [25], which is unfavorable for the protection of packaged goods and the material's durability. Rizzarelli and Carroccio [26] studied the thermo-oxidation mechanism of PBS by subjecting thin films to thermo-oxidative aging at 170 °C at different times. Combining SEC and MALDI data, they showed that PBS undergoes degradation by heat treatment in the presence of oxygen with significant molecular weight reduction and the formation of differently-terminated oligomers. As an initial step, the degradation mechanism proposed by the authors involves the extraction of hydrogen from one of the two CH_2 groups adjacent to the ester bond of the PBS chain with the formation of a hydroperoxide intermediate that decomposes with chain breakage and generation of oligomers. Usually, adding a mixture of primary antioxidants, such as sterically-hindered phenols, secondary amines, and secondary antioxidants such as peroxide decomposers [27,28], can interrupt this degradation mechanism. However, low-molecular weight antioxidants generally suffer from poor thermal stability and leaching behavior. A helpful approach to overcome this limitation is covalently binding these molecules to the polymer matrix, thereby increasing their thermal resistance and reducing the effects of migration and blooming.

Therefore, in the present paper, we studied the radical grafting reaction on PBS chains of the 3,5-di-tert-butyl-4-hydroxybenzoyl-2,2,6,6-tetramethylpiperidine-1-oxyl radical (BHB-TEMPO), a TEMPO derivative substituted with a hindered phenol unit which has the ability to scavenge peroxyl radicals by phenolic hydrogen extraction [29] (Scheme 2).

In this work, we aimed to functionalize PBS with antioxidant groups that were covalently bound to the backbone of the polymer chains and, thus, were unable to migrate. Furthermore, by exploiting the NRC reaction, we expected to limit the secondary reactions that were negatively affecting the radical functionalization processes of biopolyesters and to obtain satisfactory degrees of functionalization.
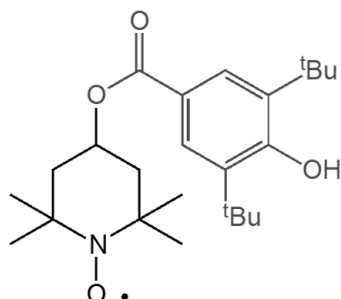
Scheme 2. Structure of 3,5-di-tert-butyl-4-hydroxybenzoyl-2,2,6,6-tetramethylpiperidine-1-oxyl radical (BHB-TEMPO).

BHB-TEMPO was grafted on PBS in solution and in a melt to assess which of the two methods yields the best results in terms of the degree of functionalization and control of secondary degradation reactions. Furthermore, the functionalized samples were characterized by size exclusion chromatography (SEC) to study any changes in molecular weight and by UV-Vis spectroscopy and proton nuclear magnetic resonance spectroscopy (^{1}H-NMR) to estimate the amount of nitroxide groups grafted onto the PBS chains. The thermal properties were evaluated by thermo-gravimetric analysis (TGA) and differential scanning calorimetry (DSC). In addition, the resistances of neat PBS and functionalized PBS versus thermo- and photo-oxidative aging were compared. Finally, a preliminary investigation of the ability of a functionalized PBS film to protect a β-carotene solution from degradation by UV-C was carried out.

2. Materials and Methods

2.1. Materials

Poly(butylene succinate) (PBS) Bionolle 1001 (Showa Highpolymer Co, Ltd., Tokyo, Japan), MFI (2.16 kg/190 °C) 1.5 g/10 min, density 1.26 g/cm^3, was dried in a vacuum oven at 80 °C for 18 h before use. Benzoyl peroxide (BPO, Sigma-Aldrich, St. Louis, MO, USA), β-carotene (synthetic, ≥93%, Sigma-Aldrich) chloroform-d (99.98% d, Sigma-Aldrich), chloroform (Carlo Erba, Milano, Italy RPE grade), chloroform HPLC grade (Sigma-Aldrich, ≥99.8%, amylene stabilized), hexane (Sigma-Aldrich, ACS reagent), and methanol (Carlo Erba, RPE grade) were used as received; 1,4-dioxane (Carlo Erba, RPE grade, 99%) was distilled over Na and stored over activated molecular sieves before use; 3,5-di-tert-butyl-4-hydroxybenzoyl-2,2,6,6-tetramethylpiperidine-1-oxyl radical (BHB-TEMPO) was available from a previous work (synthesis description and Scheme S1, Supplementary Materials) [29].

2.2. Samples Preparation

2.2.1. PBS Functionalization in Solution

Two functionalization tests were carried out in solution. In the first case, PBS (2 g) and BHB-TEMPO (0.094 g) were added to 1,4-dioxane (38 mL) in a three-neck flask. The solution was backfilled three times with nitrogen before dropwise addition of BPO (0.029 g) dissolved in 1,4-dioxane (2 mL). The solution was then heated to 95 °C and kept at this temperature while stirring for 6 h. Next, the solution was precipitated three times from methanol yielding a white powder (PBS-g-(BHB-T)1).

In the second experiment, PBS (2 g) and BHB-TEMPO (0.047 g) were added to 1,4-dioxane (36 mL) in a three-neck flask. Meanwhile, a solution of BPO (0.029 g) in 1,4-dioxane (4 mL) was prepared in a Schlenk flask. Both solutions were backfilled three times with

nitrogen. A total of 2 mL of the BPO solution was added to the three-neck flask containing the PBS/BHB-TEMPO solution previously heated to 95 °C under stirring. After 3 h, another 0.047 g of BHB-TEMPO and the remaining 2 mL of BPO solution were added to the reaction flask, keeping the system under stirring and at a constant temperature. The reaction continued for another 3 h. Next, the solution was precipitated three times into methanol, resulting in a white powder (PBS-g-(BHB-T)2).

2.2.2. PBS Functionalization in the Melt

The functionalization test in the melt was conducted in an internal batch mixer (Brabender Plastograph OHG47055, Duisburg, Germany) with a 30 mL chamber. Torque and temperature data were acquired by the Win-Mix Brabender Mixing software (ver.1.0, Duisburg, Germany). The experiment was carried out at 120 °C, with 50 rpm speed for 7 min. PBS (25 g) was introduced in the hot mixer, and BHB-TEMPO (0.588 g) was added after the melting of PBS. About 3 min after the start of the run, BPO (0.353 g) was added. The functionalized sample (PBS-g-(BHB-T)3) was dissolved in $CHCl_3$, precipitated three times from MeOH, and finally vacuum-dried to constant weight. Two additional comparison tests were carried out in Brabender. First, PBS-120 was obtained by processing 25 g of PBS at 120 °C without adding any reagent. Second, PBS-BPO was prepared by treating the 25 g of the melted polymer with 0.353 g BPO. PBS-120 was dissolved in $CHCl_3$, precipitated three times from MeOH, and vacuum dried to constant weight. PBS-BPO was only partially soluble in $CHCl_3$ and was not purified.

2.2.3. Determination of the Functionalization Degree

The functionalization degree (FD) of the PBS-g-(BHB-T) samples, representing the moles of grafted nitroxide per 100 moles of monomer repeating units of the polymer, was evaluated by UV-Vis analysis. The calibration curve was obtained by measuring the absorbance of $CHCl_3$-diluted solutions of PBS/BHB-T mixtures of known compositions. First, PBS (100 mg) was dissolved in $CHCl_3$ (10 mL), and 2.5 mL of this solution was transferred to a UV quartz cuvette. Then, small volumes of a $CHCl_3$ solution of BHB-TEMPO (6×10^{-4} M) were added gradually into the cuvette, and the UV-Vis spectrum was recorded for each solution. The absorbance at 263 nm (characteristic absorption band of BHB-TEMPO) was plotted against the BHB-TEMPO concentration (procedure description and Figure S1, Supplementary Materials). The data were subjected to linear fitting to obtain the calibration curve. The FDs of the PBS-g-(BHB-T) samples were determined by measuring the UV-Vis absorbance of sample solutions prepared by dissolving a known amount of polymer in $CHCl_3$ (Table 1). Three replicates of each sample were analyzed to determine statistical variation (average functionalization degree and relative standard deviation). In addition, the sample produced in the melt (having higher FD_{UV}) was analyzed by ^{1}H-NMR to validate the FD value.

2.3. Characterization

Thermal Gravimetric Analysis (TGA) experiments were collected on a SII ETG/DTA 7200 EXSTAR (Seiko instrument, Chiba, Japan) using 70 μL alumina sample pans. Each sample was heated at 10 °C/min from 30 to 700 °C under nitrogen flow (200 mL/min). All TGA experiments were recorded using the Muse Mobile Station software. TGA analyses were repeated three times per sample.

Differential scanning calorimetry (DSC) measurements were performed under nitrogen atmosphere (50 mL/min) on a DSC-4000 (Perkin-Elmer, Waltham, MA, USA) equipped with a 3-stage cooler able to reach −130 °C. The instrument was calibrated with indium (m.p. 156.6 °C, ΔH = 28.5 J/g) and zinc (m.p. 419.5 °C). PBS samples were heated from 30 to 150 °C at 10 °C/min (1st heating), cooled to −60 °C at the same scan rate (1st cooling), and heated again to 150 °C at 10 °C/min (2nd heating). The glass transition temperature (T_g) was measured from the inflection point in the 2nd heating thermogram. The crystallization temperature (T_c) and enthalpy (ΔH_c) were measured from the cooling

thermogram. The melting temperature (T_m) and enthalpy (ΔH_m) were measured from the 2nd heating thermogram.

Table 1. Functionalized polymer samples: feed composition, functionalization degree, and number-average molecular weight (M_n), weight-average molecular weight (M_w), and dispersity (Đ).

Sample	Feed Composition		Functionalization Degree [1] (FD)		Molecular Weight Distribution		
	BPO (mol %)	BHB-TEMPO (mol %)	FD_{UV} [2] (mol %)	FD_{NMR} [3] (mol %)	M_n [4] (g/mol)	M_w [4] (g/mol)	Đ
PBS [5]	–	–	–	–	76,000	145,200	1.9
PBS-120	–	–	–	–	72,600	147,000	2.0
PBS-BPO	1	–	–	–	n.d. [6]	n.d. [6]	n.d. [6]
PBS-g-(BHB-T)1	1	2	0.010 ± 0.003 [a]	n.d.	65,200	132,400	2.0
PBS-g-(BHB-T)2	1	2	0.014 ± 0.004 [a]	n.d.	67,400	130,700	1.9
PBS-g-(BHB-T)3	1	1 [7]	0.157 ± 0.006 [b]	0.170	65,200	137,600	2.1

[1] Functionalization Degree (FD): moles of the grafted functional groups with respect to 100 moles of monomer repeating unit. [2] Determined by the UV-Vis calibration curve. The value reported is an average of three different measurements with the corresponding standard deviation. Superscript letters (a, b) in the FD_{UV} column indicate significant differences between samples (one-way ANOVA, $p < 0.05$): similar letters in a given test indicate lack of statistically significant differences. [3] Determined by ^{1}H-NMR analysis. [4] M_n and M_w variation is about ±5%. [5] PBS pristine polymer solubilized in $CHCl_3$ and precipitated in MeOH as PBS-120, PBS-BPO, and all crude functionalized samples. [6] Not determined because the sample is partially insoluble in $CHCl_3$. [7] The amount of BHB-TEMPO used to perform this test is half that added in solution tests because, given the temperature and time conditions of the process, the maximum number of peroxide radicals produced during the run is half that obtained in solution tests.

Size exclusion chromatography (SEC) analyses were performed with an instrument consisting of a Jasco (Jasco Europe srl, Cremella (LC), Italy) PU-2089 Plus four-channel pump with degasser, a PL gel (Polymer Laboratories) pre-column packed with polystyrene/divinylbenzene, two PL gel MIXED D columns in series, thermostated in a Jasco CO-2063 column oven, a Jasco RI 2031 Plus refractive index detector, and a Jasco UV-2077 Plus multi-channel UV spectrometer. $CHCl_3$ was used as the mobile phase at a flow rate of 1 mL/min. The system was calibrated with polystyrene standards in a range from 500 to 3×10^5 g/mol. Absolute molecular weights and molecular weight distributions were calculated using the ChromNav Jasco software (ver. 2.0, Cremella (LC), Italy).

UV-Vis absorption spectra of polymer solutions were recorded at room temperature with a Perkin-Elmer Lambda 25 UV-Vis Spectrometer (Waltham, MA, USA) and with a Jasco V750 (Jasco International Co., Ltd., Tokyo, Japan).

A Bruker AV 400 (400 MHz) (Bruker, Billerica, MA, USA) equipped with a 5 mm multinuclear probe with reverse detection was used to record the ^{1}H-NMR spectra. A total of 2048 scans was recorded with an acquisition time of 5 s at 32 °C. About 40 mg of each polymer sample were dissolved in 1 mL of chloroform-d ($CDCl_3$) at room temperature and a known amount of a solution of 1,4-dinitrobenzene (reference compound, RC) in $CDCl_3$ (6.6×10^{-3} M) was added. The resulting solution was analyzed.

Films of about 60 μm thickness were obtained for each sample by compression molding using a Carver press model 4386 (Wabash, IN, USA), preheated at 120 °C and used for further analysis.

2.4. Thermal and Photo Aging

Films of the samples were exposed to heat in a static oven. Five films of each analyzed sample (10 mm × 10 mm) were placed in a Petri dish and aged at 170 °C for periods of 2, 4, 5, 6, and 7 h. Each squared film was dissolved in $CHCl_3$ and analyzed by SEC.

Films of the samples were exposed to UV radiation in a UVA Cube 400 apparatus equipped with a high-pressure mercury lamp emitting radiation in the 254–600 nm range. Samples (20 mm × 20 mm) were positioned 16 cm from the lamp and reached a temperature

of 40 °C during exposure. The exposure time was 30 and 360 min, respectively. At the end of the experiment, each sample was dissolved in CHCl₃ and analyzed by SEC.

2.5. Test of β-Carotene Protection from UV Light

A protection simulation test was conducted using a hexane solution of β-carotene as probe and two UV-C lamps with main wavelength at 254 nm and 12 W power as the irradiation source. An equal volume of probe solution was placed in UV quartz cuvettes; the cuvettes were covered with 60 μm thick PBS and PBS-g-(BHB-T)3 films, respectively, and exposed to UV radiation [30]. UV-Vis spectra were acquired at different time intervals. For comparison purposes, a quartz cell containing the probe solution was subjected to UV irradiation under the same conditions without covering the cuvette.

2.6. Statistical Analysis

Statistical analysis of FD_{UV} and TGA data was performed through variance analysis (one-way ANOVA) using OriginPro 2016 software (Northampton, MA, USA). Fisher's least significant difference at a 95% confidence level was used.

3. Results and Discussion

3.1. Preparation and Structural Characterization of Functionalized PBS Samples

The BHB-TEMPO was grafted to the PBS by the BPO-activated NRC reaction conducted in solution and in melt. Further, 1,4-dioxane was used as a solvent, operating at 95 °C. At this temperature, PBS is soluble in 1,4-dioxane, and BPO thermal decomposition occurs in a time interval that easily fits the duration of the reaction (6 h) [19]. To prepare the first sample (PBS-g-(BHB-T)1), we added BPO and BHB-TEMPO immediately after dissolution of the polymer. For the second sample (PBS-g-(BHB-T)2), we used the same quantity of reagents but we divided it into two aliquots. One aliquot was added after the dissolution of PBS, while the second was added after three hours. This procedure grants a lower instantaneous concentration of reagents compared to that of the first sample; however, the concentration of reagents is equal to that of the first sample when integrated over the total reaction time.

The functionalization reaction in the melt was carried out at 120 °C, i.e., above the melting temperature of PBS, and by adding BHB-TEMPO and BPO to the melted mass (Table 1). For comparison, we prepared two more samples: in the first case, we processed PBS alone (PBS-120) at the set temperature and, in the second case, we reacted PBS with 1 mol% of BPO (PBS-BPO) (Figure 1). For this last sample, we observed that the torque immediately increased after the addition of peroxide, indicating an increase in melt viscosity during the run. This effect is due to the coupling reaction between PBS macroradicals, formed by H-abstraction from the polymer chains (Scheme S2, Supplementary Materials). Therefore, PBS-BPO has a branched/crosslinked structure, and it is only partially soluble in CHCl₃ [18]. Indeed, this amount of peroxide was enough to obtain 60–80 wt% gel formation from the macroradical coupling reaction [31–34].

The functionalization test was carried out by adding 1 mol% of BHB-TEMPO to the melted polymer. This concentration corresponds to the maximum amount of peroxide radicals produced during the run (considering that the run was carried out for a time corresponding to the half-life time of the peroxide). The increase in torque generated by adding BPO alone was not observed in the presence of BHB-TEMPO, indicating an effective control of the PBS macroradical coupling reaction. The slight increase followed by a decrease observed in the torque graph of PBS-g-(BHB-T)3 after peroxide addition is likely attributable to a homogenization effect of the melt.
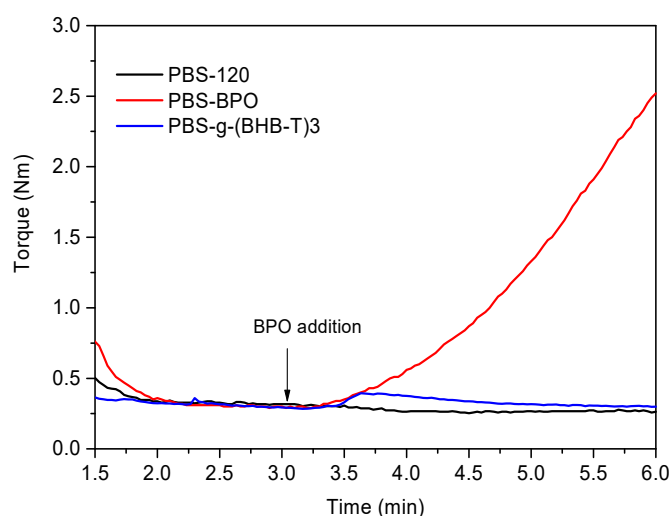
Figure 1. Torque curves of PBS-120, PBS-BPO, and PBS-g-(BHB-T)3.

SEC analysis of the functionalized samples (completely soluble in CHCl$_3$) showed a slight decrease in M$_n$ and M$_w$ compared with PBS, probably due to limited degradation (Table 1). Interestingly, this result highlights the effectiveness of BHB-TEMPO in quenching PBS macroradicals, resulting in control of the secondary reactions. Furthermore, this effect was generated both in solution and in the melt, suggesting that the process is easily scalable from a few grams (in solution) to more than 20 g (in the melt).

The grafting of BHB-TEMPO on PBS chains was confirmed by UV-Vis spectroscopy, leading to the quantitative determination of the moles of the grafted functionalities (functionalization degree, FD = moles of grafted functional groups per 100 moles of monomeric units). The characteristic absorption of BHB-TEMPO centered at 263 nm (enlargement in Figure 2), due to the π-π* transition of the aromatic ring, was observed in the spectra of the functionalized samples (Figure 2). The FD values, determined using a calibration curve constructed using standard solutions at known concentrations of PBS and BHB-TEMPO (Figure S1, Supplementary Materials), are reported in Table 1. The FD of PBS-g-(BHB-T)3 was also determined by ^{1}H-NMR spectroscopy [29,35] (analysis description and Figure S2, Supplementary Materials) to corroborate the outcomes of the UV-Vis procedure [29,35]. The result of the NMR analysis is in excellent agreement with the UV method (Table 1).
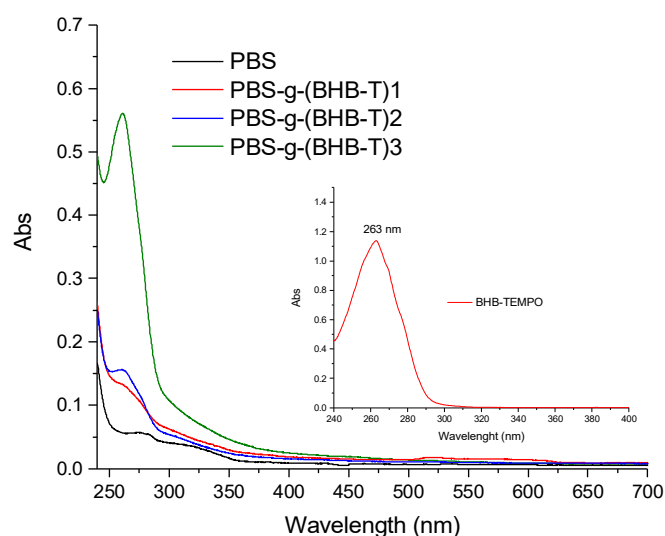

Figure 2. Representative UV-Vis absorption spectra of PBS-g-(BHB-T) samples dissolved in CHCl$_3$. The inset shows the spectrum of BHB-TEMPO (CHCl$_3$ solution).

The solution-modified samples showed 10-fold lower average FD values with respect to the PBS-g-(BHB-T)3 prepared in the melt (Table 1). Among the solution-functionalized samples, no statistically-significant difference was found in the FD values, while the difference in FD between these samples and the melt-functionalized one was statistically different. Therefore, the functionalization process carried out in the melt was more efficient in promoting the grafting reaction than that in solution [21,36]. Certainly, in the melt, the higher local concentration of the reactants compared to the polymer ensures higher efficiency. In addition, the high viscosity of the melt reduces the free movement of macroradicals and promotes their rapid quenching by BHB-TEMPO molecules. Finally, the difference in FD between melt-prepared and solution-prepared samples may be due to the transfer reaction to the solvent, which may indeed contribute to the process conducted in solution. It is also worth pointing out that the double-addition method generated a higher FD for solution-functionalized samples than the single-step method. This result suggests that the reduced instantaneous concentration of macroradicals increases the number of grafted functional groups.

The thermal properties of the functionalized samples were determined by TGA and DSC (Table 2 and Figures S3 and S4 in Supplementary Materials). The solution-functionalized samples exhibited a decrease in the thermal decomposition temperature relative to a weight loss of 5 wt% ($T_{5\%}$) compared to PBS (Table 2). This result can be attributed to the slight decrease in molecular weight observed for all samples due to the functionalization process (Table 1). However, for the sample with the highest degree of functionalization (PBS-g-(BHB-T)3), the $T_{5\%}$ value was close to that of PBS. Furthermore, the temperature corresponding to the maximum degradation rate (T_{max}) for all samples was similar, indicating that the thermal behavior is not much affected by the functionalization process.

Table 2. Thermal properties of PBS and functionalized PBS samples.

Sample	DSC [1]					TGA [2]	
	T_g (°C)	T_c (°C)	ΔH_c (°C)	T_m I/T_m II (°C)	ΔH_m (J/g)	$T_{5\%}$ (°C)	T_{max} (°C)
PBS [3]	−29.2	84.5	−79.0	105.9/116.4	77.8	346.0 ± 4.9 [a]	401.4 ± 0.1 [a]
PBS-g-(BHB-T)1	−31.1	82.9	−67.2	101.8/114.0	67.0	327.2 ± 4.6 [b]	401.2 ± 0.5 [a]
PBS-g-(BHB-T)2	−30.1	81.0	−73.0	102.8/116.2	70.4	329.5 ± 4.8 [b]	402.1 ± 0.6 [ab]
PBS-g-(BHB-T)3	−28.2	85.0	−62.0	105.6/115.4	59.4	344.0 ± 9.8 [a]	402.7 ± 0.6 [b]

[1] T_g is the glass transition temperature of PBS registered during the second heating scan; T_c is the crystallization temperature of PBS registered during the cooling; ΔH_c is the crystallization enthalpy; T_mI and T_mII are the two melting peaks of PBS observed during the second heating scan; ΔH_m is the melting enthalpy. [2] $T_{5\%}$ is the thermal decomposition temperature at 5 wt% weight loss; T_{max} is the temperature at the maximum degradation rate. The values reported are an average of three different measurements with the corresponding standard deviation. Superscript letters (a, b, and ab) in the $T_{5\%}$ and T_{max} column indicate significant differences between groups (one-way ANOVA, $p < 0.05$): similar letters in a given test indicate lack of statistically significant differences. [3] PBS was solubilized in $CHCl_3$ and precipitated in MeOH.

DSC analysis also showed very similar behavior for all of the samples, with only minor differences in the values of the fundamental thermal transitions attributable to molecular weight changes and to the presence of the grafted functional groups. The solution-functionalized samples, PBS-g-(BHB-T)1 and PBS-g-(BHB-T)2, for example, showed a lower glass transition temperature (T_g) than PBS, probably due to their lower molecular weight. In contrast, the melt-functionalized sample, PBS-g-(BHB-T)3, possessed a higher T_g value, likely due to the higher number of functional groups grafted onto the polymer chains that alter the mobility of the polymer chain segments responsible for the glass transition. In this case, the effect of the presence of functional groups balanced the slight decrease in molecular weight observed for this sample. In addition, the solution-functionalized samples had a lower crystallization temperature (T_c) than PBS, probably because of a delay in crystallization induced by a less-ordered packing of the polymer chains modified by

the side reactions. In contrast, PBS-g-(BHB-T)3 showed a T_c close to that of PBS, which could be due to the grafting onto the polymer chains of a higher number of functional groups acting as nucleants. Finally, thermograms of all samples showed a double melting peak during the second heating scan (T_mI and T_mII) ascribable to the coexistence of two crystalline populations with different lamella thickness and melting at different temperatures [37,38]. The multiple melting behavior of PBS has been discussed in the literature and ascribed to partial melting/recrystallization occurring during heating [39]. T_mII did not vary significantly from sample to sample, while T_mI was lower for PBS-g-(BHB-T)1 and PBS-g-(BHB-T)2, reflecting the T_c values. It is reported in the literature that T_mI is related to polymer crystallization during cooling and shifts toward higher values as a function of lamella thickness.

3.2. Photo- and Thermo-Oxidation Resistance of Functionalized PBS Samples

It is well-known that sterically hindered phenols substituted in para with an electron-attracting ester group are effective UV absorbers because they can act as photo-stabilizers through a Fries-type rearrangement. In addition, such phenols are effective antioxidants since they work as H-donors [40,41]. Accordingly, we investigated the antioxidant behavior of PBS functionalized with BHB-TEMPO through thermo- and photo-oxidation tests, and we compared the results with those obtained for neat PBS.

The first test was carried out by aging polymeric thin films (about 60 mm) in an oven at 170 °C for different periods of time and characterizing them by SEC. In the second experiment, the thin films were exposed to UV light for different periods and then analyzed. Figure 3 shows the trend of the number- and weight-average molecular weight of PBS and PBS-g-(BHB-T)3 aged in the oven at different times. As the thermo-oxidation time increased, both the M_n and M_w of PBS decreased significantly (Table S1, Supplementary Materials). In contrast, in the case of PBS-g-(BHB-T)3, a decrease in molecular weight was detected in the first two hours of aging, although it was less noticeable than that observed for PBS. The following hours of treatment did not result in a similarly significant change in molecular weight. The effect is particularly evident by overlapping chromatograms in the polymer elution zone (Figure S5, Supplementary Materials). The collected results thus indicate that the functional units grafted onto the polymer chains exert a stabilizing action upon thermo-oxidative aging of the PBS.
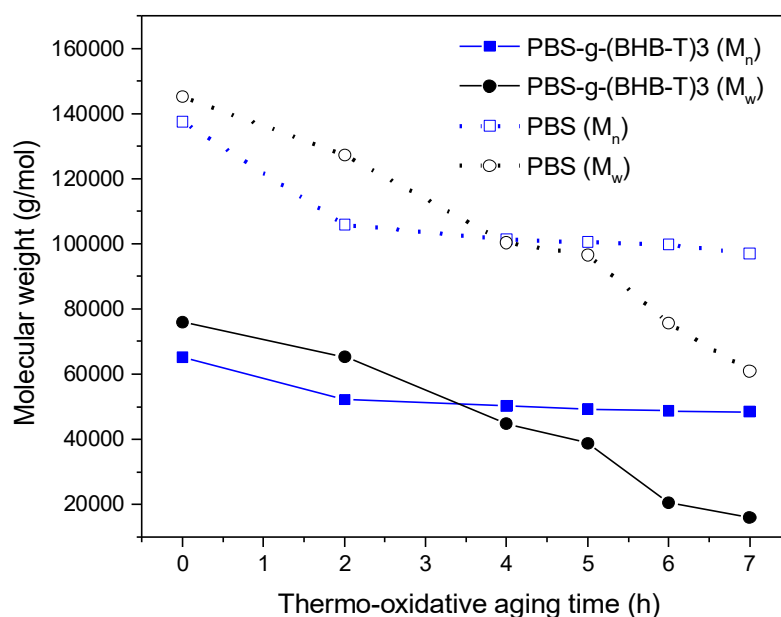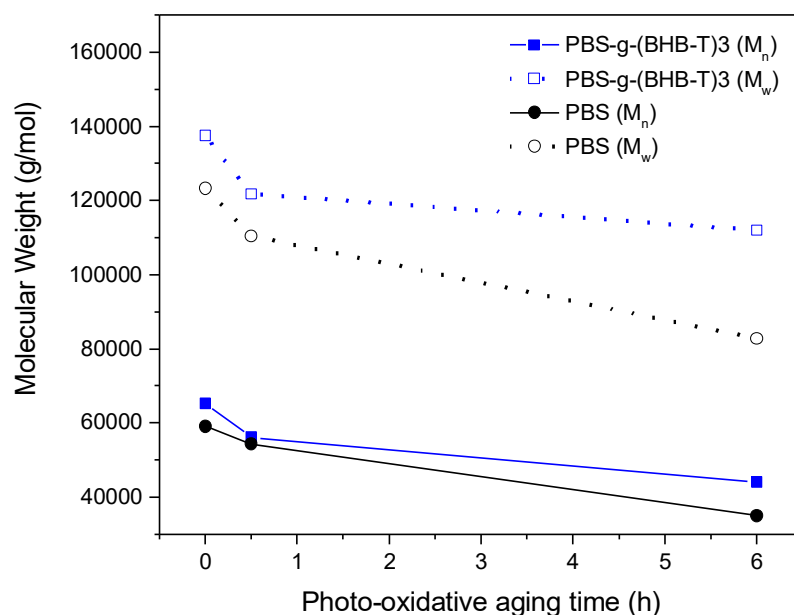

Figure 3. Number- and weight-average molecular weight of PBS and PBS-g-(BHB-T)3 as a function of thermo-oxidative aging time.

The photo-oxidation test was conducted in a UV chamber equipped with a bulb that was mainly emitting in the UV-A (330–400 nm) and UV-C (230–285 nm) regions of the electromagnetic spectrum. The SEC analysis of PBS-g-(BHB-T)3 and PBS subjected to photo-oxidative aging showed a decrease in M_n and M_w as photoirradiation time increased for both samples (Table S2 and Figure S6, Supplementary Materials); this is attributable to the degradation of the polymer chains. However, as shown in Figure 4, the decrease in molecular weight was more significant for PBS than for the functionalized sample. As in the case of thermo-oxidation, notwithstanding an initial molecular weight decrease, PBS-g-(BHB-T)3 showed better resistance to degradation in terms of molecular weight changes than PBS.

Figure 4. Number- and weight-average molecular weight of PBS and PBS-g-(BHB-T)3 as a function of photo-oxidation aging time.

3.3. UV Protection Effect of Functionalized PBS Films

Besides protecting the polymer film against UV degradation, UV-absorbing groups on PBS polymer chains can also reduce the light transmission in the UV region and protect the packaged food by blocking or absorbing UV light (UV-resistant packaging material).

Many vegetables, food, and medicines are rich in β-carotene which is very sensitive to UV light and quickly degrades when subjected to UV irradiation. Therefore, β-carotene was chosen as a probe and exposed to UV-C to simulate the irradiation of UV light on packaged goods [30]. For this purpose, the probe, consisting of a β-carotene solution, was protected with PBS and PBS-g-(BHB-T)3 films, respectively, to evaluate the extent of damage once wrapped in the two different polymer films. The variation in the maximum absorbance of β-carotene at 450 nm with irradiation time was recorded (Figure S7, Supplementary Materials). As shown in Figure 5, the absorbance of the β-carotene solution in the UV cuvette coated with the PBS film decreased over time (Figure S8, Supplementary Materials), while the coating with the PBS-g-(BHB-T)3 film protected the sample from degradation (Figure S9, Supplementary Materials). In this case, the protective effect was evident because the absorbance of β-carotene after three hours was about 80% of the initial value, while, with the PBS film, the absorbance was less than 40%. The functionalized sample, therefore, can reduce the intensity of the transmitted UV-C light, protecting β-carotene.
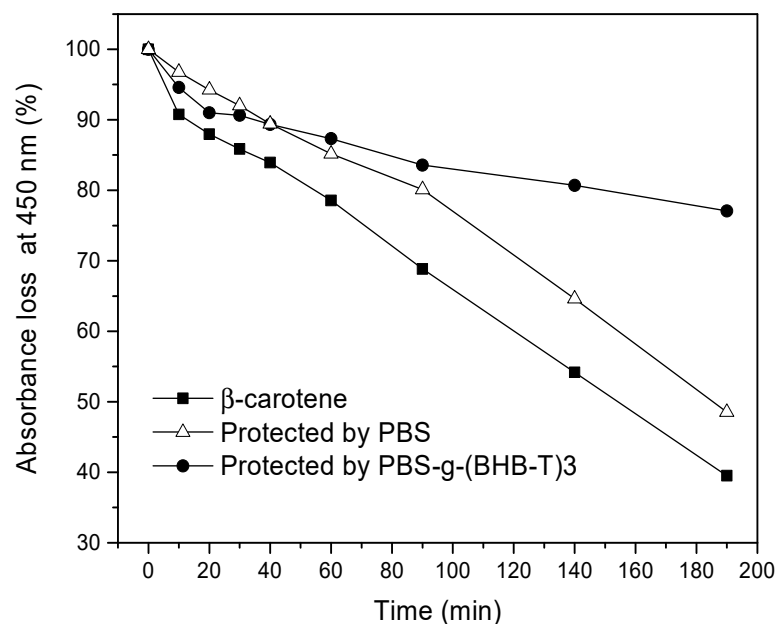
Figure 5. Absorbance loss at 450 nm of β-carotene hexane solution (10^{-5} M) alone or under the protection of PBS and PBS-g-(BHB-T)3 films as a function of irradiation time.

4. Conclusions

Grafting functional groups with antioxidant properties onto biopolyesters is crucial for the development of novel materials for active and sustainable packaging with industrial relevance. We have demonstrated an approach to synthesize functionalized PBS without incurring polymer degradation. The NRC reaction using a nitroxide derivative bearing a hindered phenol unit para-substituted with an ester group (BHB-TEMPO) allowed PBS functionalized with photo-stabilizing and antioxidant groups to be obtained.

The reaction conducted in the melt produced a higher degree of functionalization than that performed in solution, without significant changes in the polymer's molecular weight and thermal properties.

In addition, functionalized PBS demonstrated excellent stability to thermal and photo-oxidation.

Finally, a film of the modified polymer was found to protect β-carotene, a UV-sensitive molecule, from UV-induced degradation. The latter feature, combined with the excellent oxidation stability of BHB-TEMPO-functionalized PBS, makes this material (either used alone or in blends with other polyesters) suitable for sustainable and active packaging. It is biodegradable and compostable, and, at the same time, it has an adequate protective capacity. We envision that this approach will lead to the development of special polymers suitable for when protection from heat and light is required.

Supplementary Materials: The following supporting information can be downloaded at: https://www.mdpi.com/article/10.3390/compounds3010015/s1, Synthesis of BHB-TEMPO; Scheme S1: Synthesis of BHB-TEMPO; UV-Vis calibration curve for FD determination of functionalized PBS samples, Scheme S2: Simplified mechanism of BHB-TEMPO radical grafting on PBS chains, Figure S1: UV-Vis spectra of PBS/BHB-TEMPO solutions in chloroform at known concentration (a). Calibration curve (b); [1] H-NMR characterization of PBS-g-(BHB-T)3, Figure S2: ^{1}H-NMR spectra of PBS (a), and PBS-(BHB-T)3 (b). The ^{1}H-NMR spectrum of PBS shows three signals (Ha, Hb, Hc) due to the aliphatic protons of the polymer repeating units (see molecule structure in Figure S2a for attributions). The ^{1}H-NMR spectrum of PBS-g-(BHB-T)3 shows a signal (Hd) due to the aromatic protons of the grafted BHB-TEMPO unit (see molecule structure in Figure S2b for attribution). The peak at about 8.4 ppm is due to the reference compound (RC) protons, Figure S3: Representative TG (a) and DTG (b) curves of PBS, PBS-g-(BHB-T)1, PBS-g-(BHB-T)2, and PBS-g-(BHB-T)3 under nitrogen flow, Figure S4: DSC curves of PBS, PBS-g-(BHB-T)1, PBS-g-(BHB-T)2, and PBS-g-(BHB-T)3: glass transition second

heating (a); crystallization first cooling (b); melting second heating (c), Figure S5: Overlay of SEC curves between 8 and 17 min of PBS (a) and PBS-g-(BHB-T)3 (b) after 0, 2, 4, 5, 6 and 7 h of oven aging. All chromatograms were normalized, Figure S6: Overlay of SEC curves between 8 and 16 min of PBS (a) and PBS-g-(BHB-T)3 (b) after 0, 0.5, and 6 h of UV irradiation. All chromatograms were normalized, Figure S7: Overlay of UV-Vis spectra of β-carotene solution (10^{-5} M) per different irradiation time (0: 0 min; 1: 10 min; 2: 20 min; 3: 30 min; 4: 40 min; 5: 60 min; 6: 90 min; 7: 140 min; 8: 190 min), Figure S8: Overlay of UV-Vis spectra of β-carotene solution (10^{-5} M) coated with PBS film per different irradiation time (0: 0 min; 1: 10 min; 2: 20 min; 3: 30 min; 4: 40 min; 5: 60 min; 6: 90 min; 7: 140 min; 8: 190 min), Figure S9: Overlay of UV-Vis spectra of β-carotene solution (10^{-5} M) coated with PBS-g-(BHB-T)3 film per different irradiation time (0: 0 min; 1: 10 min; 2: 20 min; 3: 30 min; 4: 40 min; 5: 60 min; 6: 90 min; 7: 140 min; 8: 190 min), Table S1: Number-average molecular weight (M_n), weight-average molecular weight (M_w), and dispersity (Đ) vs. of PBS and PBS-g-(BHB-T)3 vs. the thermo-oxidative aging time, Table S2: Number-average molecular weight (M_n), weight-average molecular weight (M_w), and dispersity (Đ) of PBS and PBS-g-(BHB-T)3 vs. the photo-oxidative aging time.

References

1. RameshKumar, S.; Shaiju, P.; O'Connor, K.E. Bio-Based and Biodegradable Polymers - State-of-the-Art, Challenges and Emerging Trends. *Curr. Opin. Green Sustain. Chem.* **2020**, *21*, 75–81. [CrossRef]

2. Moshood, T.D.; Nawanir, G.; Mahmud, F.; Mohamad, F.; Ahmad, M.H.; AbdulGhani, A. Sustainability of Biodegradable Plastics: New Problem or Solution to Solve the Global Plastic Pollution? *Curr. Opin. Green Sustain. Chem.* **2022**, *5*, 100273. [CrossRef]

3. Platnieks, O.; Gaidukovs, S.; Kumar Thakur, V.; Barkane, A.; Beluns, S. Bio-Based Poly (Butylene Succinate): Recent Progress, Challenges and Future Opportunities. *Eur. Polym. J.* **2021**, *161*, 110855. [CrossRef]

4. Barletta, M.; Aversa, C.; Ayyoob, M.; Gisario, A.; Hamad, K.; Mehrpouya, M.; Vahabi, H. Poly(Butylene Succinate) (PBS): Materials, Processing, and Industrial Applications. *Prog. Polym. Sci.* **2022**, *132*, 101579. [CrossRef]

5. Jansen, M.L.A.; van Gulik, W.M. Towards Large Scale Fermentative Production of Succinic Acid. *Curr. Opin. Biotechnol.* **2014**, *30*, 190–197. [CrossRef]

6. Zheng, T.; Xu, B.; Ji, Y.; Zhang, W.; Xin, F.; Dong, W.; Wei, P.; Ma, J.; Jiang, M. Microbial Fuel Cell-Assisted Utilization of Glycerol for Succinate Production by Mutant of Actinobacillus Succinogenes. *Biotechnol. Biofuels* **2021**, *14*. [CrossRef]

7. Babaei, M.; Tsapekos, P.; Alvarado-Morales, M.; Hosseini, M.; Ebrahimi, S.; Niaei, A.; Angelidaki, I. Valorization of Organic Waste with Simultaneous Biogas Upgrading for the Production of Succinic Acid. *Biochem. Eng. J.* **2019**, *147*, 136–145. [CrossRef]

8. Brandolese, A.; della Monica, F.; Pericàs, M.À.; Kleij, A.W. Catalytic Ring-Opening Copolymerization of Fatty Acid Epoxides: Access to Functional Biopolyesters. *Macromolecules* **2022**, *55*, 2566–2573. [CrossRef]

9. Passaglia, E.; Coiai, S.; Augier, S. Control of Macromolecular Architecture during the Reactive Functionalization in the Melt of Olefin Polymers. *Prog. Polym. Sci.* **2009**, *34*, 911–947. [CrossRef]

10. Passaglia, E.; Coiai, S.; Cicogna, F.; Ciardelli, F. Some Recent Advances in Polyolefin Functionalization. *Polym. Int.* **2014**, *63*, 12–21. [CrossRef]

11. González-López, M.E.; Robledo-Ortíz, J.R.; Manríquez-González, R.; Silva-Guzmán, J.A.; Pérez-Fonseca, A.A. Polylactic Acid Functionalization with Maleic Anhydride and Its Use as Coupling Agent in Natural Fiber Biocomposites: A Review. *Compos. Interfaces* **2018**, *25*, 515–538. [CrossRef]

12. Petruš, J.; Kučera, F.; Chamradová, I.; Jančář, J. Real-Time Monitoring of Radical Grafting of Poly(Lactic Acid) with Itaconic Anhydride in Melt. *Eur. Polym. J.* **2018**, *103*, 378–389. [CrossRef]

13. Przybysz-Romatowska, M.; Haponiuk, J.; Formela, K. Reactive Extrusion of Biodegradable Aliphatic Polyesters in the Presence of Free-Radical-Initiators: A Review. *Polym. Degrad. Stab.* **2020**, *182*, 109383. [CrossRef]

14. Mani, R.; Bhattacharya, M.; Tang, J. Functionalization of Polyesters with Maleic Anhydride by Reactive Extrusion. *J. Polym. Sci. A Polym. Chem.* **1999**, *37*, 1693–1702. [CrossRef]

15. Hwang, S.W.; Lee, S.B.; Lee, C.K.; Lee, J.Y.; Shim, J.K.; Selke, S.E.M.; Soto-Valdez, H.; Matuana, L.; Rubino, M.; Auras, R. Grafting of Maleic Anhydride on Poly(L-Lactic Acid). Effects on Physical and Mechanical Properties. *Polym. Test* **2012**, *31*, 333–344.

16. Carlson, D.; Nie, L.; Narayan, R.; Dubois, P. Maleation of Polylactide (PLA) by Reactive Extrusion. *J. Appl. Polym. Sci.* **1999**, *72*, 477–485. [CrossRef]

17. Carlson, D.; Dubois, P.; Nie, L.; Narayan, R. Free Radical Branching of Polylactide by Reactive Extrusion. *Polym. Eng. Sci.* **1998**, *38*, 311–321. [CrossRef]

18. Cicogna, F.; Coiai, S.; Rizzarelli, P.; Carroccio, S.; Gambarotti, C.; Domenichelli, I.; Yang, C.; Dintcheva, N.T.; Filippone, G.; Pinzino, C.; et al. Functionalization of Aliphatic Polyesters by Nitroxide Radical Coupling. *Polym. Chem.* **2014**, *5*, 5656–5667. [CrossRef]

19. Yang, C.; Guenzi, M.; Cicogna, F.; Gambarotti, C.; Filippone, G.; Pinzino, C.; Passaglia, E.; Dintcheva, N.T.; Carroccio, S.; Coiai, S. Grafting of Polymer Chains on the Surface of Carbon Nanotubes via Nitroxide Radical Coupling Reaction. *Polym. Int.* **2016**, *65*, 48–56. [CrossRef]

20. Coiai, S.; Passaglia, E.; Cicogna, F. Post-Polymerization Modification by Nitroxide Radical Coupling. *Polym. Int.* **2019**, *68*, 27–63. [CrossRef]

21. Cicogna, F.; Coiai, S.; Passaglia, E.; Tucci, I.; Ricci, L.; Ciardelli, F.; Batistini, A. Grafting of Functional Nitroxyl Free Radicals to Polyolefins as a Tool to Postreactor Modification of Polyethylene-Based Materials with Control of Macromolecular Architecture. *J. Polym. Sci. A Polym. Chem.* **2011**, *49*, 781–795. [CrossRef]

22. Cicogna, F.; Coiai, S.; Pinzino, C.; Ciardelli, F.; Passaglia, E. Fluorescent Polyolefins by Free Radical Post-Reactor Modification with Functional Nitroxides. *React. Funct. Polym.* **2012**, *72*, 695–702. [CrossRef]

23. McLaren, M.; Jones, B.R.; Hawrylow, M.; Parent, J.S. Controlled Functionalization of Polypropylene by VETEMPO-Mediated Radical Chemistry. *Polymer* **2023**, *267*, 125651. [CrossRef]

24. Domenichelli, I.; Coiai, S.; Cicogna, F.; Pinzino, C.; Passaglia, E. Towards a Better Control of the Radical Functionalization of Poly(Lactic Acid). *Polym. Int.* **2015**, *64*, 631–640. [CrossRef]

25. Zhang, Y.; Zhou, S.; Fang, X.; Zhou, X.; Wang, J.; Bai, F.; Peng, S. Renewable and Flexible UV-Blocking Film from Poly(Butylene Succinate) and Lignin. *Eur. Polym. J.* **2019**, *116*, 265–274. [CrossRef]

26. Rizzarelli, P.; Carroccio, S. Thermo-Oxidative Processes in Biodegradable Poly(Butylene Succinate). *Polym. Degrad. Stab.* **2009**, *94*, 1825–1838. [CrossRef]

27. Reano, A.F.; Domenek, S.; Pernes, M.; Beaugrand, J.; Allais, F. Ferulic Acid-Based Bis/Trisphenols as Renewable Antioxidants for Polypropylene and Poly(Butylene Succinate). *ACS Sustain. Chem. Eng.* **2016**, *4*, 6562–6571. [CrossRef]

28. Hallstein, J.; Gomoll, A.; Lieske, A.; Büsse, T.; Balko, J.; Brüll, R.; Malz, F.; Metzsch-Zilligen, E.; Pfaendner, R.; Zehm, D. Unraveling the Cause for the Unusual Processing Behavior of Commercial Partially Bio-Based Poly(Butylene Succinates) and Their Stabilization. *J. Appl. Polym. Sci.* **2021**, *138*, 50669. [CrossRef]

29. Coiai, S.; Cicogna, F.; Yang, C.; Tempesti, V.; Carroccio, S.C.; Gorrasi, G.; Mendichi, R.; Dintcheva, N.T.; Passaglia, E. Grafting of Hindered Phenol Groups onto Ethylene/α-Olefin Copolymer by Nitroxide Radical Coupling. *Polymers* **2017**, *9*, 670. [CrossRef]

30. Ge, F.; Ding, Y.; Yang, L.; Huang, Y.; Jiang, L.; Dan, Y. Effect of the Content and Distribution of Ultraviolet Absorbing Groups on the UV Protection and Degradation of Polylactide Films. *RSC Adv.* **2015**, *5*, 70473–70481. [CrossRef]

31. Kim, D.J.; Kim, W.S.; Lee, D.H.; Min, K.E.; Park, L.S.; Kang, I.K.; Jeon, I.R.; Seo, K.H. Modification of Poly(Butylene Succinate) with Peroxide: Crosslinking, Physical and Thermal Properties, and Biodegradation. *J. Appl. Polym. Sci.* **2001**, *81*, 983–991. [CrossRef]

32. Rojas-Lema, S.; Arevalo, J.; Gomez-Caturla, J.; Garcia-Garcia, D.; Torres-Giner, S. Peroxide-Induced Synthesis of Maleic Anhydride-Grafted Poly(Butylene Succinate) and Its Compatibilizing Effect on Poly(Butylene Succinate)/Pistachio Shell Flour Composites. *Molecules* **2021**, *26*, 5927. [CrossRef]

33. Monika; Pal, A.K.; Bhasney, S.M.; Bhagabati, P.; Katiyar, V. Effect of Dicumyl Peroxide on a Poly(Lactic Acid) (PLA)/Poly(Butylene Succinate) (PBS)/Functionalized Chitosan-Based Nanobiocomposite for Packaging: A Reactive Extrusion Study. *ACS Omega* **2018**, *3*, 13298–13312. [CrossRef]

34. Campuzano, J.F.; López, I.D. Study of the Effect of Dicumyl Peroxide on Morphological and Physical Properties of Foam Injection Molded Poly(Lactic Acid)/Poly(Butylene Succinate) Blends. *Express Polym. Lett.* **2020**, *14*, 673–684. [CrossRef]

35. Hyslop, D.K.; Parent, J.S. Functional Nitroxyls for Use in Delayed-Onset Polyolefin Cross-Linking. *Macromolecules* **2012**, *45*, 8147–8154. [CrossRef]

36. Ciardelli, F.; Aglietto, M.; Pieroni, O.; Ruggeri, G.; Waymouth, R.; Kesti, M.; Stein, K. Synthetic Approaches to Functional Polymers. In *Chatgilialoglu*; Snieckus, V.C., Ed.; Chemical Synthesis. NATO ASI Series; Springer: Dordrecht, The Netherlands, 1996; Volume 320, pp. 525–548. [CrossRef]

37. Tan, L.; Chen, Y.; Zhou, W.; Ye, S.; Wei, J. Novel Approach toward Poly(Butylene Succinate)/Single-Walled Carbon Nanotubes Nanocomposites with Interfacial-Induced Crystallization Behaviors and Mechanical Strength. *Polymer* **2011**, *52*, 3587–3596. [CrossRef]
38. Yasuniwa, M.; Satou, T. Multiple Melting Behavior of Poly(Butylene Succinate). I. Thermal Analysis of Melt-Crystallized Samples. *J. Polym. Sci. B Polym. Phys.* **2002**, *40*, 2411–2420. [CrossRef]
39. di Lorenzo, M.L.; Androsch, R.; Righetti, M.C. Low-Temperature Crystallization of Poly(Butylene Succinate). *Eur. Polym. J.* **2017**, *94*, 384–391. [CrossRef]
40. Allen, N.S.; Kotecha, J.L.; Parkinson, A.; Loffelman, F.F.; Rauhut, M.M.; Susi, P.V. Photo-Stabilising Action of a p-Hydroxybenzoate Light Stabiliser in Polyolefins: Part III—Antioxidant Behaviour and Additive/Pigment Interactions in High Density Polyethylene. *Polym. Degrad. Stab.* **1985**, *10*, 1–13. [CrossRef]
41. Allen, N.S.; Edge, M. Perspectives on Additives for Polymers. Part 2. Aspects of Photostabilization and Role of Fillers and Pigments. *J. Vinyl Addit. Technol.* **2021**, *27*, 211–239. [CrossRef]